Chemical Science

ROYAL SOCIETY OF CHEMISTRY

EDGE ARTICLE

View Article Online
View Journal | View Issue

Cite this: *Chem. Sci.*, 2024, **15**, 11783

All publication charges for this article have been paid for by the Royal Society of Chemistry

Received 17th May 2024
Accepted 13th June 2024

DOI: 10.1039/d4sc03232b

rsc.li/chemical-science

Total synthesis, biological evaluation and biosynthetic re-evaluation of *Illicium*-derived neolignans†

Robert E. Arnold,[a] Jan Saska,[a] Raquel Mesquita-Ribeiro,[b] Federico Dajas-Bailador,[b] Laurence Taylor,[a] William Lewis,[a] Stephen Argent,[a] Huiling Shao,[c] Kendall N. Houk *[c] and Ross M. Denton *[a]

We report the first total syntheses of simonsol F (**3**), simonsinol (**5**), fargenin (**4**), and macranthol (**6**) in addition to syntheses of simonsol C (**2**), simonsol G (**1**), and honokiol (**14**). The syntheses are based upon a phosphonium ylide-mediated cascade reaction and upon natural product isomerization reactions which proceed through Cope rearrangements of putative biosynthetic dienone intermediates. As a corollary of the natural product isomerization reactions, we propose an alternative biosynthesis of honokiol (**14**), simonsinol (**5**), and macranthol (**6**) which unites the natural products in this family under a single common precursor, chavicol (**7**). Finally, we demonstrate that simonsol C (**2**) and simonsol F (**3**) promote axonal growth in primary mouse cortical neurons.

Introduction

Plants of the genus *Illicium* have long been a rich source of natural products. For example, the seed pod of *Illicium verum* is star anise, a common flavoring, while the fruit of the same plant is a traditional Chinese medicine used for the treatment of abdominal pain. More recently *Illicium*-derived natural products have attracted considerable attention because of their potent neurotrophic properties.[1,2] Depicted in Fig. 1 are two groups of neolignans [3] that are of interest as a result of their molecular structures, biosynthetic origin and potential biological activity. The first group (Fig. 1A) contains the skeletally distinct metabolites simonsol G (**1**),[4] simonsol C (**2**),[5] simonsol F (**3**)[6] and fargenin (**4**),[7] which share a *cis*-fused tetrahydrodibenzofuran ring system as their central structural element. The second group (Fig. 1B) contains the constitutionally isomeric aromatic sesquineolignans simonsinol (**5**)[8] and macranthol (**6**).[9] The first group is of particular interest because of their structural resemblance to the galantamine alkaloids[10] and synthetic analogs such as narwedine (**8**, Fig. 1C), which is used in the clinic for the symptomatic treatment of Alzheimer's disease.[11] This similarity was noted by Banwell and co-workers who reported the first synthesis of racemic simonsol C (**2**) in 2016.[12] This was followed by a second total synthesis which was very recently disclosed by Qin and co-workers.[13] Banwell's observation, coupled with the fact that several structurally related neolignans have been shown to exhibit neuroprotective effects,[14–19] stimulated our interest in this family, and analogs thereof, as a possible source of new neuroprotective compounds.

Biosynthetic analysis

Alongside potential biological activity, we were intrigued by the biosynthetic origins of these natural products. For example, the compounds depicted in Fig. 1A are homooligomers likely derived from the natural product chavicol (**7**) and a plausible biosynthesis (Scheme 1A) involves oxidation and deprotonation of **7** (ref. 20 and 21) to generate radical **9** followed by *ortho–ortho* dimerization giving magnolol (**10**). From this branch point the trimeric natural products can be reached as follows. Oxidative coupling of magnolol (**10**) and chavicol (**7**) according to Path A gives dienone **13** and, following conjugate addition, simonsol C (**2**). An alternative oxidative coupling (Path B, Scheme 1) generates dienone **11**, a second branch point, from which simonsol F (**3**) and fargenin (**4**) are derived through conjugate addition and addition/dehydration reactions respectively. Experimental support for these pathways comes from Brown and co-workers who have demonstrated that a variety of natural products including magnolol (**10**) and simsonol G (**1**) were formed non-selectively and in low yield when chavicol (**7**) was treated with iron trichloride.[22]

In contrast simonsinol (**5**) and macranthol (**6**) (Scheme 1B) are *prima facie* heterooligomers derived from chavicol (**7**) and the additional phenolic precursor (**15**) through a presumed

[a]*The GlaxoSmithKline Carbon Neutral Laboratories for Sustainable Chemistry, University of Nottingham, Jubilee Campus Triumph Road, Nottingham, NG7 2TU, UK. E-mail: ross.denton@nottingham.ac.uk*

[b]*School of Life Sciences, University of Nottingham, NG7 2UH, UK*

[c]*University of California, Department of Chemistry and Biochemistry, 607 Charles E. Young Drive East, Box 951569, Los Angeles, CA 90095-1569, UK*

† Electronic supplementary information (ESI) available. CCDC 2327688–2327695. For ESI and crystallographic data in CIF or other electronic format see DOI: https://doi.org/10.1039/d4sc03232b

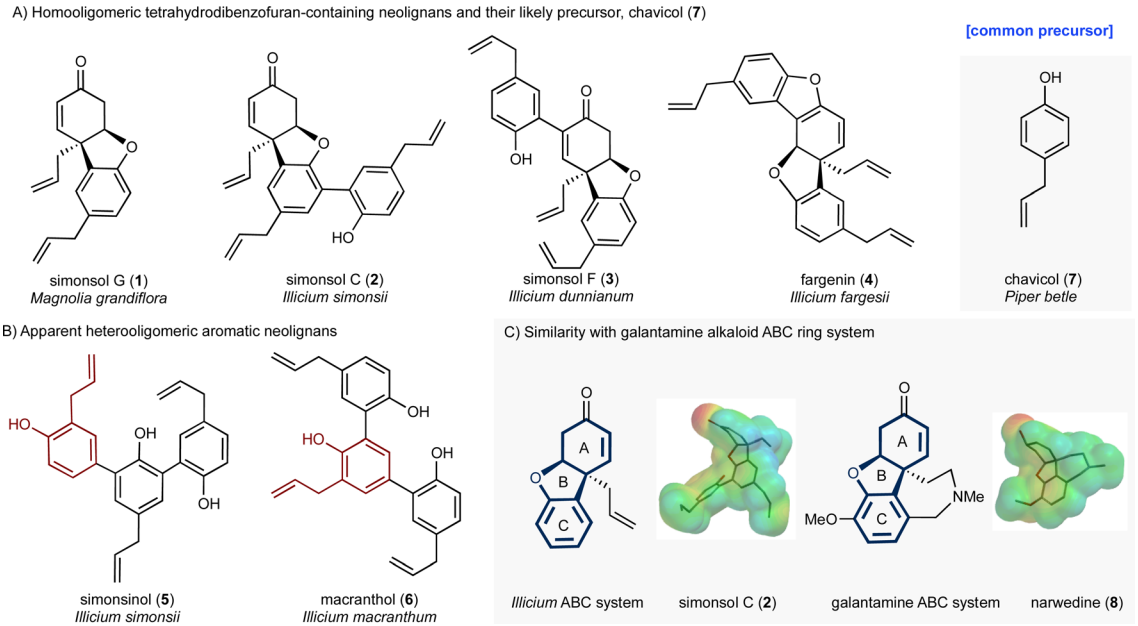

Fig. 1 Structures of *Illicium*-derived neolignan natural products.

oxidative coupling which generates the natural product honokiol (**14**).[23–28] From this point macranthol (**6**) and simonsinol (**5**) can be reached following further oxidative coupling with chavicol (**7**) as indicated (Scheme 1B).

However, while chavicol (**7**) and its methylated counterpart estragole have been isolated from numerous plants, including basil, fennel, and star anise (*Illicum verum*),[29] phenol **15** is very scarce indeed.[30] Furthermore, honokiol (**14**) is typically isolated with the homodimer magnolol (**10**) suggesting a common origin from chavicol (**7**) which undermines the presumed oxidative coupling of **7** and **15** depicted in Scheme 1B.[31]

Synthesis plan

In order to explore the biological activity and possible biosynthesis of these *Illicium* natural products we designed a method for the construction of the core [4.3.0] tetrahydrodibenzofuran ring system (Scheme 1C) featuring intermediate **16**, with appropriate substituents X and Y, as a key building block. In principle **16** should be accessible from a cascade reaction in which a phosphonium ylide mediates a ring-opening, conjugate addition and methylenation sequence (**19** →**18**→**17**→**16**, Scheme 1C). The cascade precursor **19** should be available through a dearomatizing spirocyclization reaction[32] of biaryl **20**, itself derived from cross-coupling of **21** and **22**. Any such cross-coupling is potentially complicated by thermodynamic isomerization of the terminal alkenes. However, we have previously completed the total synthesis of simple aromatic neolignans[33–35] and shown that, with care, cross-coupling and deprotection reactions could be carried out efficiently. Furthermore, we also investigated the proposed cascade reaction and demonstrated its feasibility on a simple model system, albeit with limited success.[36]

Herein we report total syntheses of simonsol C (**2**), simonsol F (**3**) and simonsol G (**1**) based upon the successful implementation of this general approach. Additional syntheses of simonsinol (**5**), fargenin (**4**), macranthol (**6**), and honokiol (**14**) through isomerization processes provide evidence for a new biosynthesis proposal which unites the neolignans in Fig. 1 under a single common precursor. Finally, using neuronal models, the potential connection between neolignans and galantamine alkaloids is explored and tetrahydrodibenzofuran-containing neolignans are shown to promote axonal growth.

Results and discussion

Total synthesis of simonsol C (2) and simonsol F (3)

The synthesis of simonsol C (**2**) (Scheme 2) began with the preparation of boronic acid **24** through *ortho*-lithiation of **23** followed by quenching with trimethylborate and transesterification with pinacol. Subsequent treatment with boron trichloride dimethylsulfide complex effected cleavage of the methyl ether and pinacol ester and gave the boronic acid **24** and dimer **25** in a combined yield of 47% over three steps.

Suzuki–Miyaura cross-coupling of this mixture with bromide **26** then gave biaryl **27** which was brominated to afford intermediate **28** from which acetal **29** was prepared by reaction with bromine and ethyl vinyl ether. A dilute solution of **29** was then treated with cesium fluoride, which resulted in silyl ether cleavage and spirocyclization to afford dienone **30**, the structure of which was confirmed by X-ray analysis.

Having reached this stage we sought hydrolysis conditions that would convert **30** into the corresponding hemi-acetal **33** required for the cascade reaction (Scheme 1C). Following some experimentation, we found that treatment of **30** with aqueous hydrochloric acid gave 28% of the desired hemiacetal **33** along with enone **32** (6%) and inseparable ketone diastereomers **31** (50%) which had arisen through post hydrolysis oxa-1,4-addition reactions. While hemiacetal **33** was not obtained as the major product it was available following chromatography

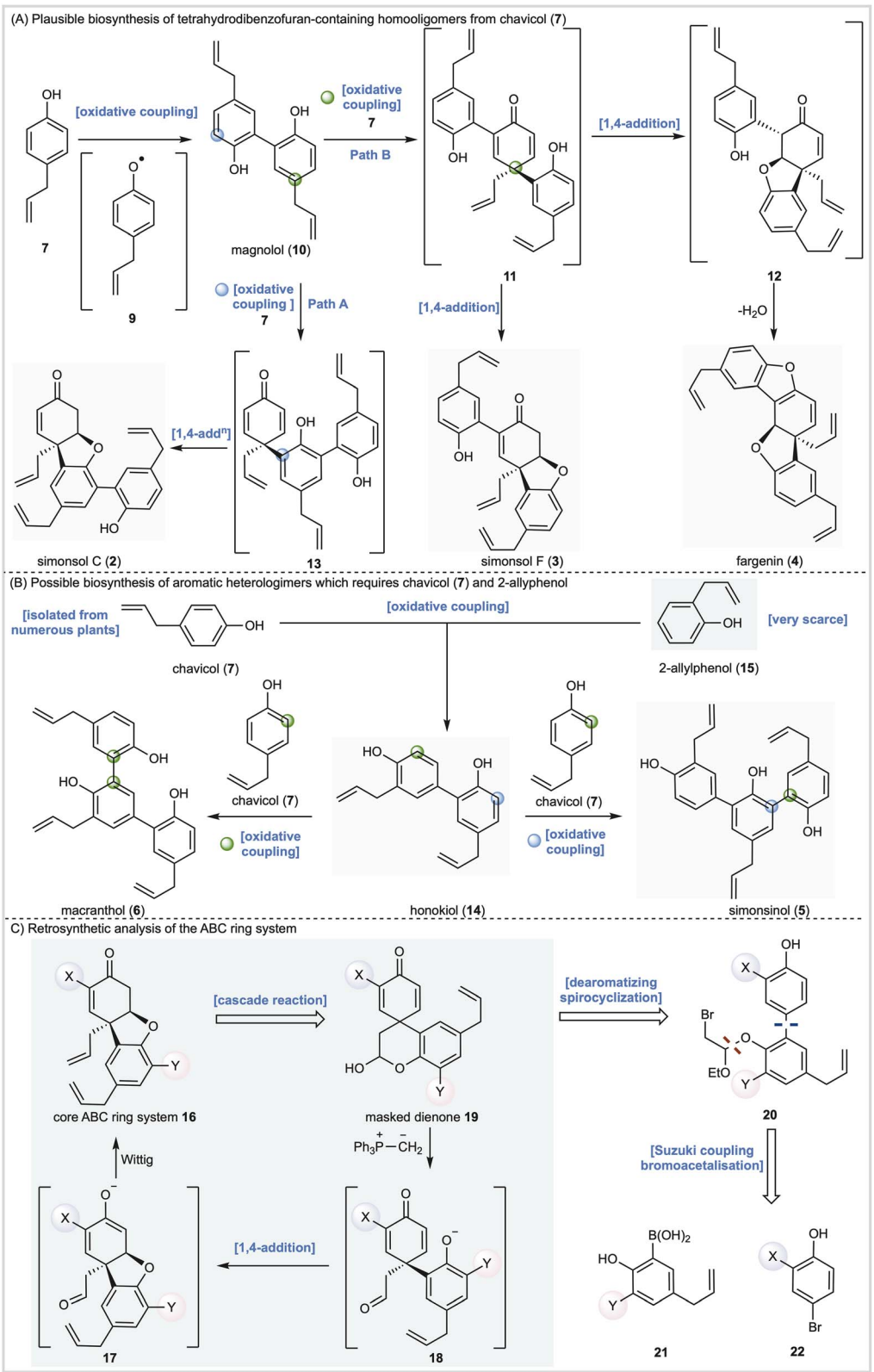

Scheme 1 Proposed biosynthesis and retrosynthetic analysis of *Illicium* neolignans.

and so we proceeded to examine the planned cascade reaction. To this end **33** was treated with methylenetriphenylphosphorane and the desired tricyclic intermediate **34** was obtained in an excellent 90% isolated yield and the structure of this material was confirmed by X-ray crystallography (Scheme 2C).

Although our synthesis plan had now been validated through the successful conversion of **33** into **34**, we had to face the

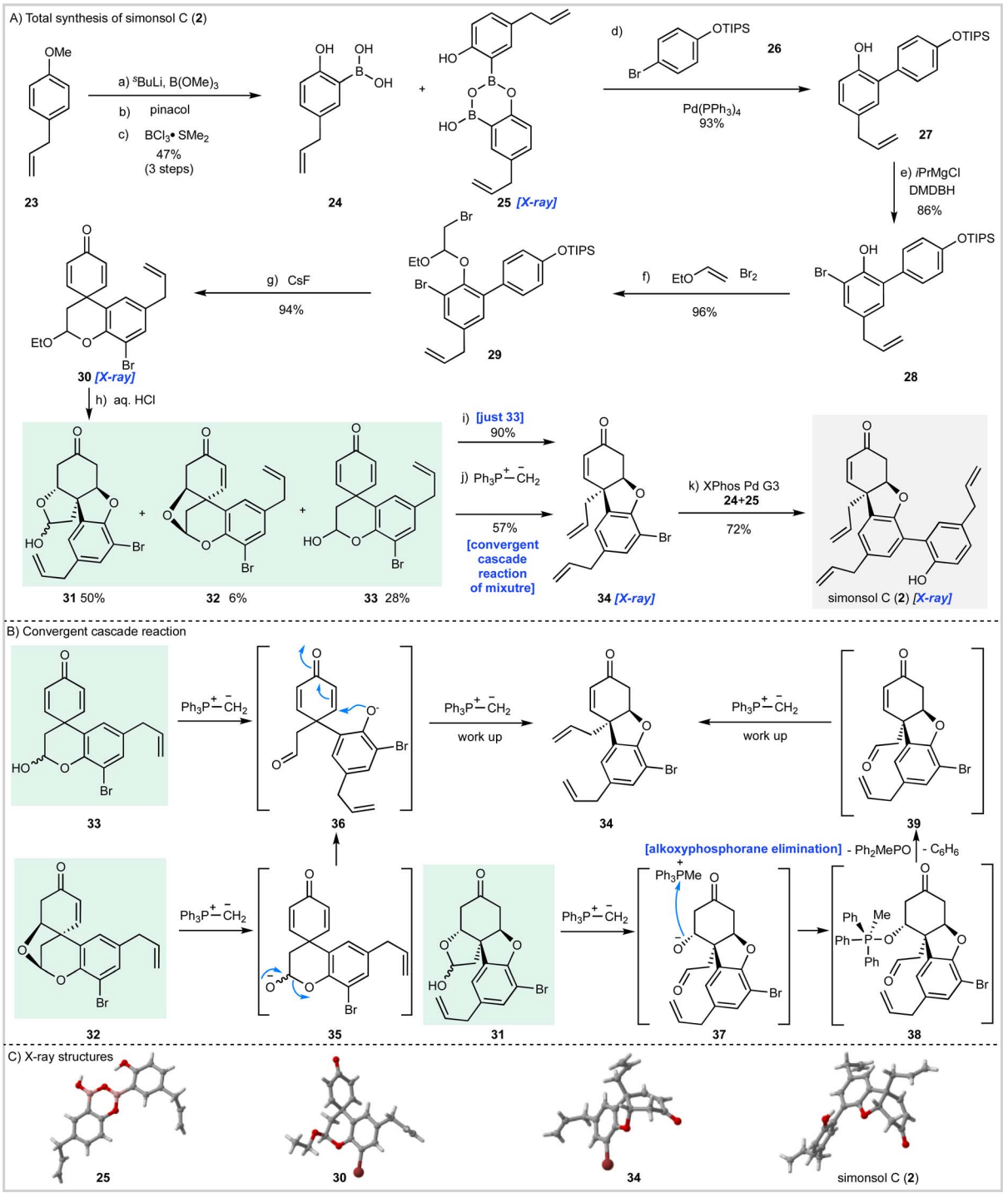

Scheme 2 Total synthesis of simonsol C (**2**). (A) Reagents and conditions: (a) *s*BuLi, $B(OMe)_3$, TMEDA, THF, −78 °C to r.t., 1 h; (b) pinacol, methanol, r.t., 16 h; (c) $BCl_3 \cdot SMe_2$, 1,2-DCE, 80 °C, 16 h, 47% (3 steps); (d) $Pd(PPh_3)_4$ (8 mol%), aq. Na_2CO_3, THF, r.t. 1.5 h, 93%; (e) DBDMH, *i*PrMgCl, THF, − 78 °C to r.t., 1.5 h, 86%; (f) ethyl vinyl ether, Br_2, Hünig's base, DCM, 0 °C to r.t., 2.5 h, 96%; (g) CsF, Na_2SO_4, DMF, 130 °C, 1 h, 94%; (h) HCl aq., 1,4-dioxane, 80 °C, 10.5 h, **33** 28%, **32** 6%, **31** 50%; (i) $MePPh_3$ Br, KHMDS, THF, 0 °C, 1 h, 90% (just **33**); (j) $MePPh_3Br$, KHMDS, THF, 0 °C, 1 h, 57% (convergent cascade reaction of mixture); (k) XPhos Pd G3 10 mol%, aq. K_3PO_4, THF, 50 °C, 1.3 h, 72%. (B) Convergent cascade reaction pathways. (C) X-ray structures. THF = tetrahydrofuran, TMEDA = *N*,*N*,*N*′,*N*′-tetramethylethylenediame, DBDMH = dibromo dimethyl hydantoin, DMF = dimethylformamide, KHMDS = potassium hexamethyldisilazide.

problem that hemiacetal **33** was only available as the minor product from the hydrolysis of acetal **30**. To develop a viable synthesis of simonsol C (**2**) a means of recycling or, ideally, progressing the other hydrolysis products **31** and **32** was required. Since these by-products had arisen through conjugate addition, we reasoned it might be possible to effect β-elimination reactions under the basic conditions of the cascade reaction and thereby develop a process under which the hydrolysis products

converge. Fortunately, this proved to be the case, and when a mixture of **31**, **32** and **33** were treated with the phosphonium ylide we were delighted to isolate product **34** in 57% yield. We believe that this convergent process occurs as shown in Scheme 1B. It is likely that dienone **33** and enone **32** converge to give aldehyde **36** through deprotonation and ring-opening in the case of **33** and β-elimination/ring-opening in the case of **32**. Subsequent conjugate addition of **36** and methylenation then gives product **34** after work up. In the case of the inseparable ketone diastereoisomers **31**, deprotonation results in ring-opening to give alkoxide **37** which then forms alkoxyphosphorane intermediate **38** (ref. 37) after alkoxide addition to the phosphonium salt. Elimination of this intermediate to generate **39** may then proceed by an E_1cB mechanism resulting in the generation of methyldiphenylphosphine oxide and benzene.

With a viable cascade sequence now developed we examined the Suzuki–Miyaura coupling reaction to access simonsol C (**2**). As expected, this proved challenging and was complicated by: (a) the free hydroxyl group present within the boronic acid; (b) isomerization of the allyl groups; and (c) additional reactions of the natural product which occurred post cross-coupling (*vide infra*). After numerous experiments, in which a wide range of palladium pre-catalysts were examined, an efficient cross-coupling was realized using Buchwald's third generation palladacycle XPhos Pd G3 (ref. 38) which gave simonsol C (**2**) in a 72% isolated yield. The structure of our synthetic material was confirmed by X-ray crystallography (Scheme 2C).

Having now fully validated our synthesis strategy we next turned our attention to simonsol F (**3**) which, prior to our work, had not been synthesized (Scheme 3A). To this end biaryl **40** was prepared by Suzuki–Miyaura coupling of the appropriate aryl halide and a mixture of boronic acids **24** and **25** (see ESI†). The biaryl then underwent bromoacetalization to give **41** followed by desilylation and spirocyclization to give an inconsequential mixture of bromodienone diastereoisomers **42**, whose structures were confirmed by X-ray crystallography (Scheme 3C). Unfortunately, progressing either the single dienone isomers or the mixture through the required acetal hydrolysis proved to be extremely challenging. A range of conditions were examined, all of which gave intractable mixtures of debrominated material. As a result, we were forced to explore Suzuki–Miyaura cross-coupling prior to hydrolysis of the cyclic acetal. In our initial experiments we established that separate diastereoisomers of **42** underwent efficient coupling with boronic acid ester **43** (not depicted) before developing a more efficient method for cross-coupling of the mixture (Scheme 3A) which gave **44** as a mixture of diastereoisomers in excellent yield.

We now had to develop hydrolysis conditions to obtain hemiacetal **45** for deployment in the cascade reaction. In this instance, when mixture **45** was heated with aqueous hydrochloric acid under the conditions used for the synthesis of simonsol C (**2**) a complex mixture of products was obtained. However, acid-catalyzed hydrolysis using camphorsulfonic acid gave hemiacetal **45** as the major product in an acceptable yield of 66%. Treatment of this mixture with methylenetriphenylphosphorane again proceeded smoothly to give methyl-protected simonsol F (**47**) establishing this sequence as a general method for the construction of functionalized tetrahydrodibenzofurans. In this iteration of the cascade reaction, the presumed dienone phenolate intermediate **46**, or its methylenated equivalent, can undergo conjugate 1,4-addition at two sites (Scheme 3B). Experimentally, formation of simonsol F (**3**) *via* intermediate **47** was observed and QM calculations suggested that the site selectivity is thermodynamically controlled. The alternative conjugate addition products **49** and **50** are 2.3 and 5.4 kcal mol^{-1} higher in energy respectively than **47**. This is consistent with nucleophilic attack on the more electron-deficient enone, not substituted by the electron-rich aromatic substituent. This reaction also preserves the conjugation of this substituent to the double bond, stabilizing the product.

As with simonsol C (**2**) the final step of the synthesis proved to be challenging as a result of the sensitive allyl groups and the reactivity of the natural product post deprotection. After considerable experimentation we identified demethylation conditions that involved treatment of **48** with BCl_3 at 0 °C for 5.5 hours which gave simonsol F (**3**) in an excellent isolated yield of 85% (Scheme 3A). The structure of the natural product was confirmed by X-ray crystallography (Scheme 3C).

Synthesis of fargenin (4), macranthol (6), simonsinol (5), and honokiol (14) through natural product isomerization

During the syntheses of simonsol F (**3**) and simonsol C (**2**), we had observed that both natural products were thermally unstable to the extent that cross-coupling and demethylation conditions had to be carefully developed to avoid generating additional products. Therefore, we next explored the innate reactivity of these natural products and our notion that dienone intermediates *e.g.* **11** (Scheme 1A), serve as biosynthetic branch points. If such intermediates could be accessed from the natural products themselves through retro conjugate addition, it would provide evidence for our biosynthesis, as well as opening isomerization pathways between natural products. Gratifyingly this reasoning proved to be correct, and we discovered that when simonsol F (**3**) was heated in toluene at 100 °C, it was converted into the pentacyclic natural product fargenin (**4**, 29%), the triaryl natural product macranthol (**6**, 15%) and benzofuran **48** (23%) (Scheme 3A). This remarkable series of transformations provides compelling evidence for intermediate **11** and the divergent reactivity associated with the cross-conjugated dienone moiety.

As depicted in Scheme 3A the formation of these products can be rationalized by invoking retro conjugate addition to generate dienone **11**. Fargenin (**4**) is then obtained through 1,2-addition of the phenolic hydroxyl group followed by dehydration, as indicated by the blue label on intermediate **11**. An alternative oxidative 1,4-addition reaction (pink-labelled carbon) gives rise to benzofuran **48**, and a Cope rearrangement (green label) is responsible for the generation of macranthol (**6**). The Cope rearrangement is of potential biosynthetic significance as it provides a hitherto unknown pathway to macranthol (**6**) which we had previously assumed to be a heterooligomer originating from the oxidative coupling of chavicol (**7**) and 2-allylphenol (**15**) (Scheme 1B).

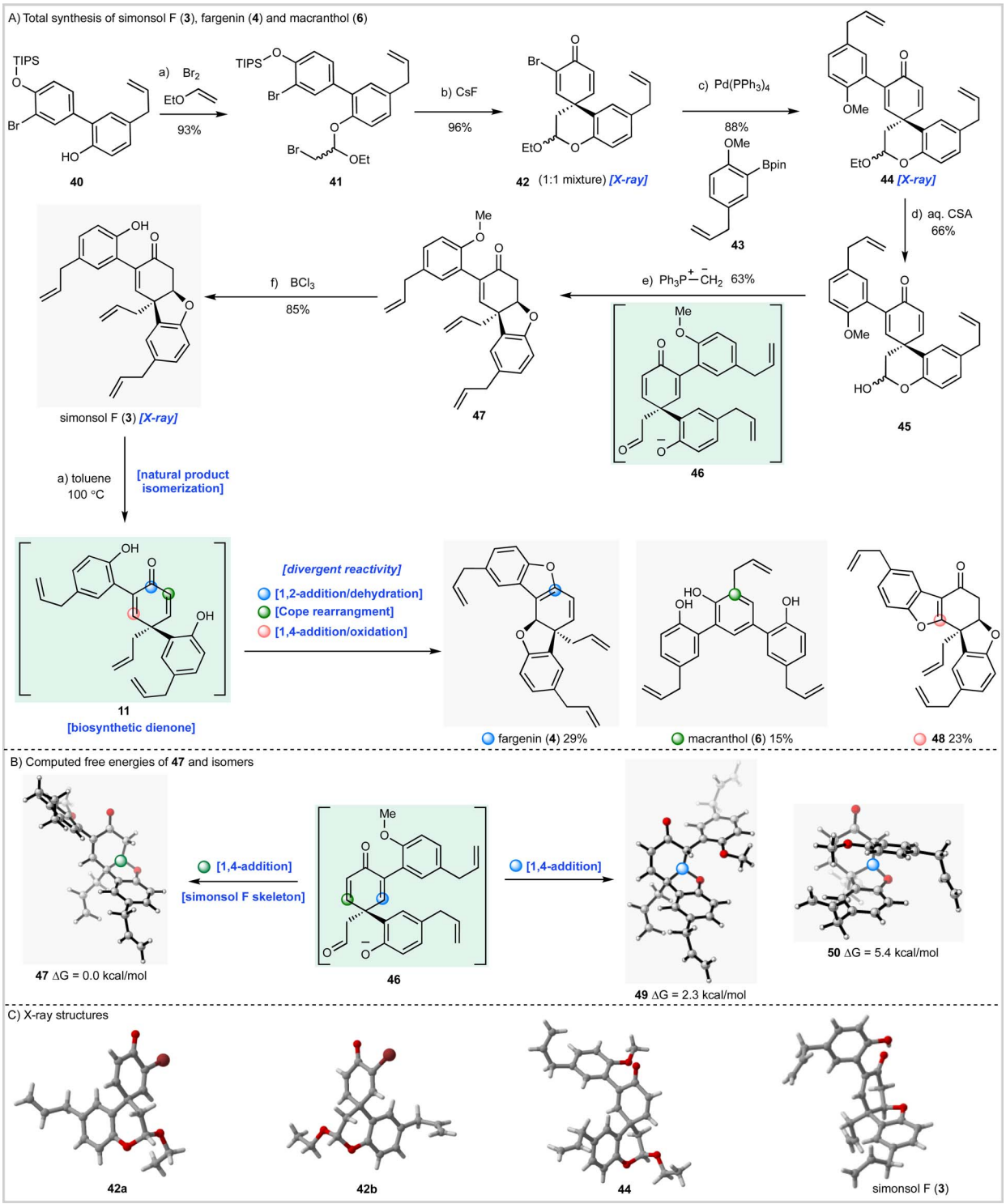

Scheme 3 Total synthesis of simonsol F (**3**) and its possible biomimetic conversion into fargenin (**4**) and macranthol (**6**). (A) Reagents and conditions: (a) ethyl vinyl ether, Br_2, Hünig's base, DCM, 0 °C to r.t., 2.5 h, 93%; (b) CsF, Na_2SO_4, DMF, 130 °C, 1 h, 96%; (c) $Pd(PPh_3)_4$, aq. Na_2CO_3, toluene°:°ethanol, 85 °C, 4 h, 88%; (d) CSA, H_2O, 1,4-dioxane, 85 °C, 10.5 h, 66%; (e) $MePPh_3Br$, KHMDS, THF, 0 °C, 0.5 h, 63%; (f) BCl_3, DCM, 0 °C, 5.5 h, 85%; (a) toluene-d_8, 100 °C, 228 h, macranthol (**6**) 15%, fargenin (**4**) 29%, **58** 23%. (B) Computed free energies of **47** and isomers. (C) X-ray structures. DCM = dichloromethane, CSA = camphorsulfonic acid.

Given these observations we next sought to effect isomerization of other homooligomeric natural products into their presumed heterooligomeric aromatic counterparts (Scheme 4A). In agreement with the results described above we discovered that simonsol G (**1**), which was prepared using our cascade strategy (see ESI† for the synthesis), could be converted into honokiol (**18**)

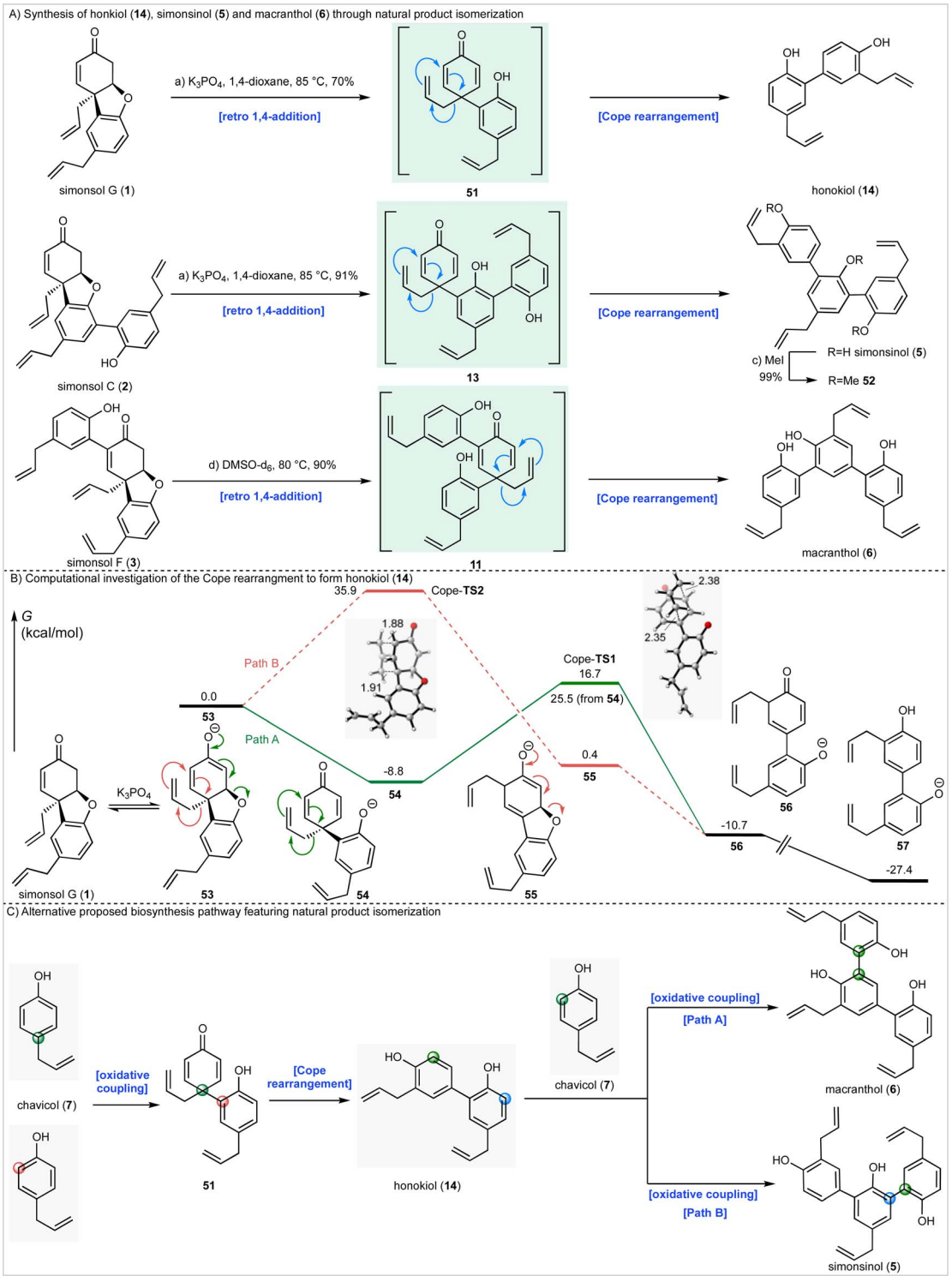

Scheme 4 Synthesis of honokiol (**14**), simonsinol (**5**) and macranthol (**6**) through natural product isomerization. (A) Reagents and conditions: (a) K_3PO_4, 1,4-dioxane, 85 °C, 40 h, 70% (b) K_3PO_4 aq., THF, 80 °C, 7 h, 91%; (c) MeI, K_2CO_3, acetone, 55 °C, 24 h, 99%; (d) DMSO-d6, 85 °C, 16 h, 90%. (B) Computational analysis of potential Cope rearrangements. (C) Alternative biosynthesis proposal. DMSO = dimethylsulfoxide.

under mild basic conditions. Similarly, simonsol C (**2**) and simonsol F (**3**) were converted into simonsinol (**5**) and macranthol (**6**) respectively. In the case of simoninsol (**5**), permethylation to give ether **52** was carried out for comparison with the literature compound derived from natural simonsinol (**5**).

To gain further insight into the Cope rearrangements we conducted DFT calculations to study the isomerization process that converts simonsol G (**1**) into honokiol (**14**). In the presence of base, this likely occurs through the generation of an equilibrium concentration of enolate **53** which could proceed

through either Path A or Path B (Scheme 4B), depending on the order of the retro conjugate addition and Cope rearrangement. Path A, as invoked in Scheme 4A, involves a retro-conjugate addition of simonsol G enolate **53** to form the dienone intermediate **54**, which undergoes Cope rearrangement and tautomerization to form anionic honokiol **57**. Alternatively, along Path B, Cope rearrangement of **53** forms the dienolate intermediate **55**, which then undergoes retro-conjugate addition and tautomerization to form **56**. For completeness, we also investigated the corresponding neutral Cope rearrangements leading to honokiol (**14**) and macranthol (**6**) (see ESI†). Our computed reaction coordinate profile of Path A suggests that the formation of the dienone intermediate **54** from the simonsol G enolate **53** is exergonic by 8.8 kcal mol^{-1} (Scheme 4B). The subsequent Cope rearrangement transition state (Cope-TS1) has a relatively low free energy barrier of 25.5 kcal mol^{-1}, and formation of the rearrangement product **56** is exergonic by 1.9 kcal mol^{-1}. Subsequent tautomerization forms the honokinol phenolate **57**, which is exogonic by 18.6 kcal mol^{-1}.

Alternatively, Path B (Scheme 4B) *via* Cope-TS2 has a high free energy barrier of 35.9 kcal mol^{-1}, which is kinetically unlikely at the reaction temperature (85 °C). Both Cope

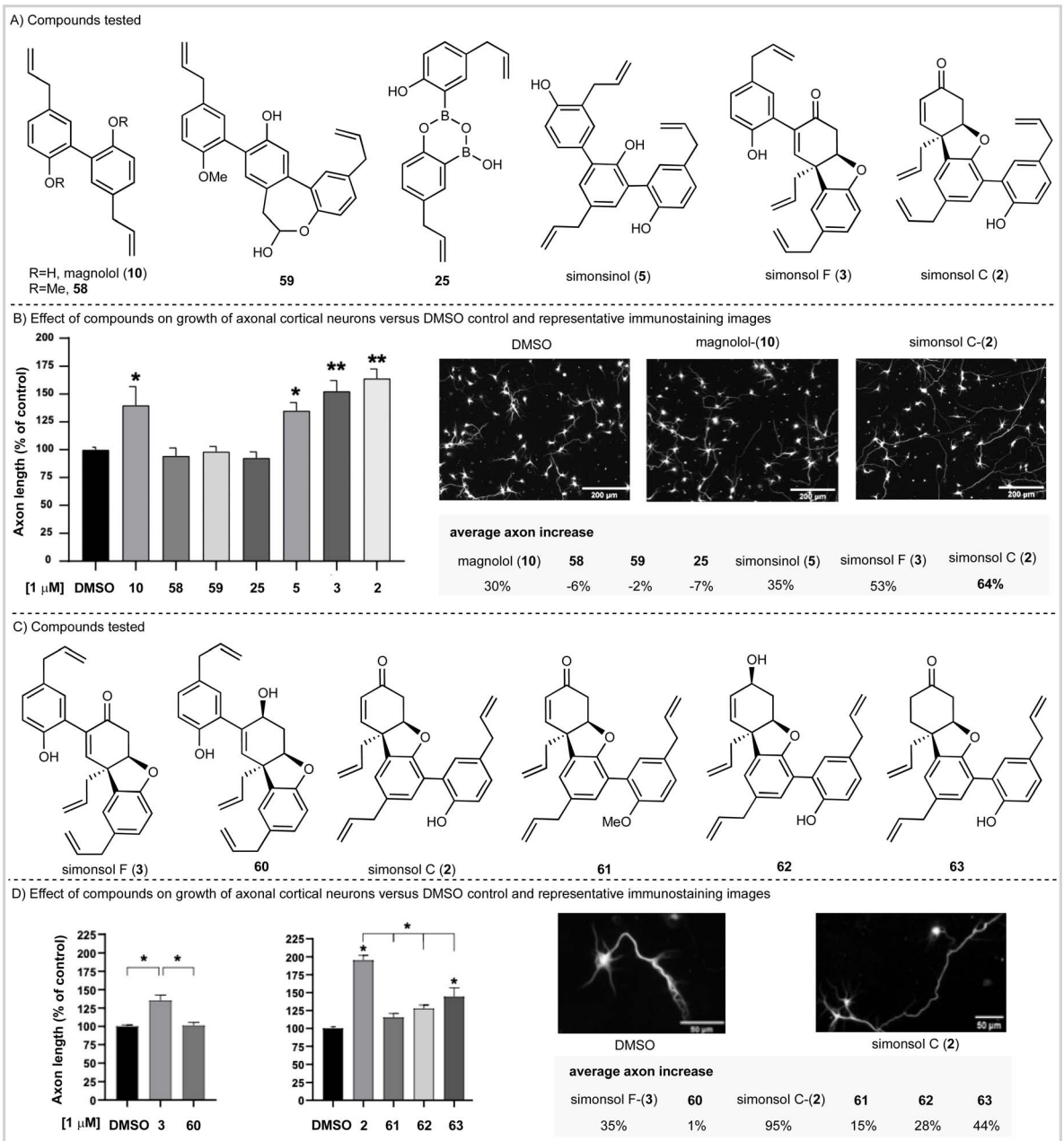

Scheme 5 Effect of *Illicium* natural products and analogs on axonal growth. (A and C) Compounds tested. (B and D) Analysis of the effect of *Illicium*-derived neolignans and intermediate compounds on the growth of the axon of primary cortical neurons 48 hours after incubation in culture, as compared to control DMSO. Data obtained from 3–5 independent experiments, ~160–200 axons measured per condition in each; *$p < 0.05$, **$p < 0.01$, one-way ANOVA with posthoc Dunnet's multiple comparison test.

transition states adopt the favored chair-like conformation (Scheme 4B). As a result of the cross conjugated nature of dienone **54** the Cope-TS1 is favored over Cope-TS2 by 19.2 kcal mol^{-1}. Based on these calculations we conclude that the natural product conversions take place through the proposed biosynthetic dienones **51**, **13** and **11**, or corresponding anions depending on the reaction conditions (Scheme 4A).

Biosynthetic ramifications

The isomerization processes that we have discovered and elucidated above have important consequences for the likely biosynthetic origin of honokiol (**14**), simonsinol (**5**), and macranthol (**6**). Specifically, it is no longer necessary to view these natural products as heterooligomers. Instead, we can draw a revised biosynthesis with chavicol (**7**) as the sole precursor (Scheme 4C). We suggest that honokiol arises from an *ortho-para* oxidative coupling of chavicol (**7**) to generate dienone **51** which can undergo a Cope rearrangement to generate honokiol (**14**) (Scheme 4C). Subsequent oxidative coupling with chavicol (**7**) can now generate macranthol (**6**) (Path A) or simonsinol (**5**) (Path B).

Alternatively, honokiol (**14**), simonsinol (**5**) and macranthol (**6**) could arise from the isomerization processes that we have demonstrated experimentally (Scheme 4A) with the formation of an additional aromatic ring as the thermodynamic driving force. Although the calculated barrier of the Cope rearrangement of **54** is relatively high ($t_{1/2}$ 6 days at 25 °C), it is possible that this could be accelerated through enzyme catalysis. Examples of enzymes catalyzing pericyclic reactions are rare;[39] however, there is evidence to support biosynthetic Cope rearrangements in alkaloid biosynthesis[40–42] and there are biogenetically inspired syntheses of other *Illicium* natural products which feature Claisen and Cope rearrangements.[43]

Biological investigations: axonal growth assay

Having completed our total synthesis studies, we sought to investigate the potential neuronal functional properties of tetrahydrodibenzofuran-containing *Illicium* neolignans. When simonsol C (**2**) was isolated and characterized by Wang and coworkers, no anti-acetylcholinesterase activity was observed *in vitro* (no inhibition below 100 μM) nor was any anti-butyrylcholinesterase activity observed (no inhibition below 50 μM). However, Banwell suggested that the similarity between the ABC rings of simonsol C (**2**) and galantamine alkaloids (Fig. 1C) was such that biological investigation for the former was warranted.[12]

The fact that both magnolol (**10**), which is contained within simonsol C (**2**), and honokiol (**14**) have been shown to possess neuroprotective and restorative effects[44–46] lends credence to this notion. As does the additional observations that a variety of structurally related neolignans and sesquiterpene neoligans exhibit neurite outgrowth properties.[14–19,47,48] Given that axonal functional loss and degeneration is known to occur at the early stages of neurodegenerative diseases which precedes cell death and the onset of clinical symptoms[49] we opted to screen compounds in an axonal growth assay. We began by examining magnolol (**10**), simonsinol (**5**), simsonol C (**2**), and simonsol F (**3**) along with selected synthetic intermediates **58**, **59** and **25** which contained phenolic, phenylpropenoid and ether moieties (Scheme 5A). The compounds were applied as DMSO solutions to primary embryonic mouse cortical neurons that had been cultured for two days on poly-L-ornithine coated glass coverslips. Following a forty-eight-hour incubation, neurons were fixed and immunostained for the axonally-enriched acetylated tubulin to reveal overall neuron morphology. Each coverslip was imaged at 20 random points and the axonal length of neurons was measured computationally (Scheme 5B).

This study established that magnolol (**10**), simonsinol (**5**), simonsol F (**3**) and simonsol C (**2**) increased the length of mouse primary cortical axons at 1 μM. Furthermore, simonsol F (**3**) and simonsol C (**2**) promoted axonal growth at a level above that of the dimeric and trimeric aromatic natural products magnolol (**10**) and simonsinol (**5**) (Scheme 5B). Therefore, the galantamine alkaloid-like tetrahydrodibenzofuran core is biologically relevant in the promotion of axonal growth.

To gain further insight, we prepared a range of novel analogs (see SI for synthesis) in order to further probe the role of the tetrahydrodibenzofuran core (Scheme 5C). We began by examining simonsol F (**3**) and its reduced counterpart **60** at a concentration of 1 μM (Scheme 5D). The allylic alcohol **60** did not promote axonal growth, which illustrates the requirement for the enone within the tetrahydrodibenzofuran ring system. A second comparison between simonsol C-(**2**) and derivatives **61**, **62** and **63** was then made (Scheme 5C and D). These results show that, in the case of simonsol C (**2**), a free phenol and the enone are required for the significant axonal growth which is observed. Taken together these data support Banwell's suggestion that simonsol C (**2**), and analogs thereof, may be promising starting points for the development of novel small molecules of therapeutic relevance in neurodevelopmental and neurodegenerative diseases.

Conclusion

In this Article we have documented the first total synthesis of simonsol F (**3**), simonsinol (**5**), fargenin-(**4**), macranthol (**6**) and reported additional total syntheses of simonsol C (**2**), simonsol G (**1**), and honokiol (**14**). The syntheses were based upon a phosphonium ylide-mediated cascade reaction which allowed for the efficient construction of the characteristic [4.3.0] core ring system, and upon natural product isomerization reactions which feature unusual dienone Cope rearrangements. As a corollary of the rearrangement processes, we proposed an alternative biosynthetic origin of honokiol (**14**), simonsinol (**5**) and macranthol (**6**), from a single common precursor chavicol (**7**). Finally, we have shown that both simonsol C (**2**) and simonsol (**F**) promote axonal growth and that the enone-containing tetrahydrodibenzofuran ring system is required for this activity.

Data availability

The experimental and computational data supporting this article have been included as part of the ESI.†

Author contributions

R. M. D. conceived the work. R. M. D. and R. E. A. prepared the manuscript. The synthesis work was carried out by R. E. A. and J. S. and R. E. A., J. S., and R. M. D. analysed the data. The computational chemistry was carried out by H. S. and K. N. H. The X-ray crystallography was carried out by S. A., L. T., and W. L. The axonal growth assays and subsequent data analysis was carried out by R. M.-B. and F. D.-J.

Conflicts of interest

There are no conflicts of interest to declare.

Acknowledgements

Mice (C57/BL6) for primary neuron cultures were housed, bred and sacrificed (Schedule 1) in compliance with the ethics and animal welfare in accordance with the Animal (Scientific Procedures) Act 1986, which is in place at the University of Nottingham, UK. We acknowledge financial support from the School of Chemistry, University of Nottingham (PhD Studentship to R. E. A. and J. S.).

Notes and references

1 J. Xu, M. H. Lacoske and E. A. Theodorakis, *Angew. Chem., Int. Ed.*, 2014, **53**, 956–987.
2 J. Richers, A. Pöthig, E. Herdtweck, C. Sippel, F. Hausch and K. Tiefenbacher, *Chem.–Eur. J*, 2017, **23**, 3178–3183.
3 Y. Yang, Z. Wang, J. Wu and Y. Chen, *Chem. Biodiversity*, 2016, **13**, 269–274.
4 A. Latif, Y. Du, S. R. Dalal, M. L. Fernández-Murga, E. F. Merino, M. B. Cassera, M. Goetz and D. G. I. Kingston, *Chem. Biodiversity*, 2017, **14**, e1700209.
5 C. Dong, L. Liu, X. Li, Z. Guan, H. Luo and Y. Wang, *Planta Med.*, 2013, **79**, 338–347.
6 L. K. Sy and G. D. Brown, *Phytochemistry*, 1996, **43**, 1417–1419.
7 M. Moriyama, J.-M. Huang, C.-S. Yang, H. Hioki, M. Kubo, K. Harada and Y. Fukuyama, *Tetrahedron*, 2007, **63**, 4243–4249.
8 I. Kuono, T. Morisaki, Y. Hara and C.-S. Yang, *Chem. Pharm. Bull.*, 1997, **117**, 415–434.
9 I. Kuono, A. Hashimoto, K. Nobusuke and C.-S. Yang, *Chem. Pharm. Bull.*, 1989, 1291–1292.
10 J. Marco-Contelles, M. do Carmo Carreiras, C. Rodríguez, M. Villarroya and A. G. García, *Chem. Rev.*, 2006, **106**, 116–133.
11 S. Majumder, A. Yadav, S. Pal, A. Khatua and A. Bisai, *J. Org. Chem.*, 2022, **87**, 7786–7797.
12 J. Nugent, M. G. Banwell and B. D. Schwartz, *Org. Lett.*, 2016, **18**, 3798–3801.
13 J. J. Sui, K. Wang, S. J. Luo, K. Guo, M. W. Yuan and H. B. Qin, *J. Org. Chem.*, 2024, 7821–7827.
14 X. Cheng, N. L. Harzdorf, T. Shaw and D. Siegel, *Org. Lett.*, 2010, **12**, 1304–1307.
15 Z. Khaing, D. Kang, A. M. Camelio, C. E. Schmidt and D. Siegel, *Bioorg. Med. Chem. Lett.*, 2011, **21**, 4808–4812.
16 Y. Fukuyama, K. Nakade, Y. Minoshima, R. Yokoyama, H. Zhai and Y. Mitsumoto, *Bioorg. Med. Chem. Lett.*, 2002, **12**, 1163–1166.
17 T. Esumi, G. Makado, H. Zhai, Y. Shimizu, Y. Mitsumoto and Y. Fukuyama, *Bioorg. Med. Chem. Lett.*, 2004, **14**, 2621–2625.
18 Y. Fukuyama, Y. Otoshi, K. Miyoshi, K. Nakamura, M. Kodama, M. Nagasawa, T. Hasegawa, H. Okazaki and M. Sugawara, *Tetrahedron*, 1992, **48**, 377–392.
19 K. Zlotkowski, J. Pierce-Shimomura and D. Siegel, *ChemBioChem*, 2013, **14**, 307–310.
20 G. Brunow, I. Kilpeläinen, J. Sipilä, K. Syrjänen, P. Karhunen, H. Setälä and P. Rummakko, *ACS Symp. Ser.*, 1998, **697**, 131–147.
21 S. C. Tzeng and Y. C. Liu, *J. Mol. Catal. B: Enzym.*, 2004, **32**, 7–13.
22 L. K. Sy and G. D. Brown, *J. Chem. Res.*, 1998, 476–477.
23 R. M. Denton, J. T. Scragg, A. M. Galofré, X. Gui and W. Lewis, *Tetrahedron*, 2010, **66**, 8029–8035.
24 P. R. Khan, T. Mujawar, P. Shekhar, G. Shankar, B. V. Subba Reddy and R. Subramanyam, *Tetrahedron Lett.*, 2020, **61**, 152229–152230.
25 A. M. Wright and G. W. O'Neil, *Tetrahedron Lett.*, 2016, **57**, 3441–3443.
26 K. Harada, C. Arioka, A. Miyakita, M. Kubo and Y. Fukuyama, *Tetrahedron Lett.*, 2014, **55**, 6001–6003.
27 C. M. Chen and Y. C. Liu, *Tetrahedron Lett.*, 2009, **50**, 1151–1152.
28 T. Esumi, G. Makado, H. Zhai, Y. Shimizu, Y. Mitsumoto and Y. Fukuyama, *Bioorg. Med. Chem. Lett.*, 2004, **14**, 2621–2625.
29 J. K. Patra, G. Das, S. Bose, S. Banerjee, C. N. Vishnuprasad, M. del Pilar Rodriguez-Torres and H. S. Shin, *Phytother Res.*, 2020, **34**, 1248–1267.
30 M. Arumugam, A. Mitra, P. Jaisankar, S. Dasgupta, T. Sen, R. Gachhui, U. Kumar Mukhopadhyay and J. Mukherjee, *Appl. Microbiol. Biotechnol.*, 2010, **86**, 109–117.
31 F. Amblard, D. Delinsky, J. L. Arbiser and R. F. Schinazi, *J. Med. Chem.*, 2006, **49**, 3426–3427.
32 P. Magnus, N. Sane, B. P. Fauber and V. Lynch, *J. Am. Chem. Soc.*, 2009, **131**, 16045–16047.
33 R. M. Denton and J. T. Scragg, *Synlett*, 2010, **4**, 633–635.
34 R. M. Denton, J. T. Scragg and J. Saska, *Tetrahedron Lett.*, 2011, **52**, 2554–2556.
35 R. M. Denton, J. T. Scragg, A. M. Galofré, X. Gui and W. Lewis, *Tetrahedron*, 2010, **66**, 8029–8035.
36 R. M. Denton and J. T. Scragg, *Org. Biomol. Chem.*, 2012, **10**, 5629–5635.
37 P. A. Byrne and D. G. Gilheany, *Chem.–Eur. J.*, 2016, **22**, 9140–9154.
38 N. C. Bruno, M. T. Tudge and S. L. Buchwald, *Chem. Sci.*, 2013, **4**, 916.
39 K. N. Houk, X.-S. Xue, F. Liu, Y. Chen, X. Chen and C. Jamieson, *Isr. J. Chem.*, 2022, **62**, e202100071.
40 H. P. Chen and I. Abe, *Synth. Syst. Biotechnol.*, 2021, **6**, 51–62.
41 S. A. Newmister, S. Li, M. Garcia-Borràs, J. N. Sanders, S. Yang, A. N. Lowell, F. Yu, J. L. Smith, R. M. Williams,

K. N. Houk and D. H. Sherman, *Nat. Chem. Biol.*, 2018, **14**, 345–351.
42 L. Y. P. Luk, Q. Qian and M. E. Tanner, *J. Am. Chem. Soc.*, 2011, **133**, 12342–12345.
43 J. A. Homer, I. De Silvestro, E. J. Matheson, J. T. Stuart and A. L. Lawrence, *Org. Lett.*, 2021, **23**, 3248–3252.
44 C. P. Hoi, Y. P. Ho, L. Baum and A. H. L. Chow, *Phytother Res.*, 2010, **24**, 1538–1542.
45 H. H. Chen, S. C. Lin and M. H. Chan, *Neurodegener. Dis.*, 2011, **8**, 364–374.
46 N. Matsui, K. Takahashi, M. Takeichi, T. Kuroshita, K. Noguchi, K. Yamazaki, H. Tagashira, K. Tsutsui, H. Okada, Y. Kido, Y. Yasui, N. Fukuishi, Y. Fukuyama and M. Akagi, *Brain Res.*, 2009, **1305**, 108–117.
47 Z. Khaing, D. Kang, A. M. Camelio, C. E. Schmidt and D. Siegel, *Bioorg. Med. Chem. Lett.*, 2011, **21**, 4808–4812.
48 Y. Fukuyama, M. Kubo and K. Harada, *J. Nat. Med.*, 2020, **74**, 648–671.
49 N. Salvadores, M. Sanhueza, P. Manque and F. A. Court, *Front. Neurosci.*, 2017, **11**, 451.